NIH Public Access
Author Manuscript
J Med Chem. Author manuscript; available in PMC 2010 December 1.

Published in final edited form as:
J Med Chem. 2009 December 10; 52(23): 7868–7872. doi:10.1021/jm900576g.

High lipophilicity of *meta* Mn(III) *N*-alkylpyridylporphyrin-based SOD mimics compensates for their lower antioxidant potency and makes them equally effective as *ortho* analogues in protecting SOD-deficient *E. coli*

Ivan Kos[1,a], **Ludmil Benov**[2], **Ivan Spasojević**[3], **Júlio S. Rebouças**[1,b], and **Ines Batinić-Haberle**[1,*]

[1] Department of Radiation Oncology, Duke University Medical School, Durham, NC 27710, USA

[2] Department of Biochemistry, Faculty of Medicine, Kuwait University, Safat 13110, Kuwait

[3] Department of Medicine, Duke University Medical School, Durham, NC 27710, USA

Abstract

Lipophilicity/bioavailibility of Mn(III)*N*-alkylpyridylporphyrin-based SOD mimics has major impact on their *in vivo* ability to suppress oxidative stress. *Meta* isomers are less potent SOD mimics than *ortho* analogues, but are 10-fold more lipophilic and more planar. Enhanced lipophilicity contributes to their higher accumulation in cytosol of SOD-deficient *E. coli*, compensating for their lower potency; consequently both isomers exert similar-to-identical protection of SOD-deficient *E. coli*. Thus *meta* isomers may be as prospective therapeutics as are *ortho* porphyrins.

Keywords

Meta and *ortho* isomers of Mn(III) *N*-alkylpyridylporphyrins; SOD-deficient *E. coli* protection; accumulation of Mn porphyrins in *E. coli*; SOD mimics; peroxynitrite scavengers; MnTM-2-PyP; MnTE-2-PyP^{5+}; MnTnHex-2-PyP; MnTM-3-PyP; MnTE-3-PyP

Introduction

Positively charged Mn(III) *N*-alkylpyridylporphyrins (Figure 1) display electrostatic and thermodynamic facilitation for the dismutation of superoxide ($O_2^{\cdot-}$) and reduction of peroxynitrite ($ONOO^-$).[1–4] Some members of the series are among the most potent catalytic scavengers of these reactive species with activity towards $O_2^{\cdot-}$nearly the same as that of the SOD enzymes,[4] and reactivity towards $ONOO^-$, k_{red} exceeding 10^7 M^{-1} s^{-1}.[3] Reactive species are widely viewed as signaling molecules controlling cellular transcriptional activity.[5] Thus, inhibition of the activation of redox-active transcription factors such as AP-1,[6] NF-kB,[7,8] and HIF-1α[9–11], presumably *via* scavenging of reactive species, was detected by

*Corresponding author: Ines Batinić-Haberle, Ph. D., Department of Radiation Oncology-Cancer Biology, Duke University Medical Center, Research Drive, 281b/285 MSRB I, Box 3455, Durham, NC 27710, Tel: 919-684-2101; Fax: 919-684-8718, ibatinic@duke.edu.

[a]Present Addresses for *Julio S. Reboucas*: Departamento de Química, CCEN, Universidade Federal da Paraíba, Caixa Postal 5093, João Pessoa, PB, 58051-970, Brazil, and for *Ivan Kos*: Faculty of Pharmacy and Biochemistry, University of Zagreb, A. Kovacica 1, 10 000 Zagreb, Croatia.

Supplemental Information is available on *J. Med. Chem.* web site.

NIH-PA Author Manuscript
NIH-PA Author Manuscript
NIH-PA Author Manuscript

NIH-PA Author Manuscript

NIH-PA Author Manuscript

NIH-PA Author Manuscript

some members of the series. Mn porphyrins, such as MnTE-2-PyP, MnTnHex-2-PyP, and MnTDE-2-ImP, effectively attenuate oxidative stress in animal models of cancer,[6,9–11] central nervous system disorders,[8] radiation injury,[12] diabetes,[7,13] morphine tolerance,[14] ischemia/reperfusion injuries[16] etc. Recent data, however, has hinted that factors other than redox-based antioxidant potency, such as lipophilicity, size, and the overall geometry and conformational flexibility of the Mn porphyrins (MnP) should play also a significant role in their design and activity.[4,15,17]

In our seminal work published in 1998,[18] the magnitude and the importance of the lipophilicity for the *in vivo* SOD-like efficacy of MnP, as well as the remarkable gain in lipophilicity (at the expense of activity) by the mere shift of the alkyl group from an *ortho* onto a *meta* position could only have been retrospectively speculated. Recently, we were able to overcome the methodological difficulties associated with the determination of the partition coefficients between n-octanol and water, P_{OW}. The P_{OW}, as opposed to TLC retention factor, R_f, is a common and practical indicator of drug lipophilicity which allows comparison of MnP to other drugs of similar target (Table 1).[17] We observed that, whereas R_f is linearly related to log P_{OW}, small differences in R_f translate into considerable difference in log P_{OW}.[17] We further showed that a ~10-fold gain in lipophilicity is achieved by either (**1**) moving the alkyl groups on *meso* pyridyl substituents from *ortho* to *meta* positions, or (**2**) by increasing the length of alkyl chains by one CH_2 group (Table 1).[17] Thus, MnTnHex-2-PyP and MnTnOct-2-PyP are, respectively, ~13,000- and ~460,000- fold more lipophilic than MnTE-2-PyP. Whereas these compounds share roughly the same antioxidant capacity (as given by their log k_{cat} values), the 120- and 3000-fold increase in *in vivo* efficacy of MnTnHex-2-PyP[12,16,20,22,23] and MnTnOct-2-PyP[20,21](relative to MnTE-2-PyP) in animal and cellular models of oxidative stress seems to be due, at least in part, to their increased lipophilicity and therefore increased cellular accumulation. Among several different classes of metal compounds studied (Mn cyclic polyamines, Mn salens, different MnP and $MnCl_2$ as a control), only MnTnHex-2-PyP protects ataxia telangiectasia cells against radiation damage in a first study to show that both bioavailability and antioxidant capacity are essential for *in vivo* drug efficacy.[23] In a rabbit model of cerebral palsy MnTnHex-2-PyP, and not hydrophilic MnTE-2-PyP, rescued puppies.[23] Due to the exceptional antioxidant potential of *ortho* isomeric Mn *N*-alkylpyridylporphyrins in dismuting $O_2^{\cdot-}$ and reducing $ONOO^-$, we[1–4] and others[24] have been extensively studying them and analogues *ortho*-substituted corroles.[25]

The ~10-fold increase in the lipophilicity of the *meta* as compared to *ortho* isomers may compensate for their inferior antioxidant potency making them prospective therapeutics. Further, the rotational flexibility of the *meta* isomers when compared to conformational rigidity of the *ortho* isomers may affect favorably their cellular uptake and sub-cellular biodistribution. We thus decided to revisit *meta* isomers to better describe the factors that contribute to the *in vivo* efficacy of these seemingly different MnP. For *in vivo* studies we employed our simple and convenient $O_2^{\cdot-}$-specific model that relies on the aerobic growth of SOD-deficient *E. coli*. Thus far, it has always been a reliable predictor of a prospective drug candidate.[18,20]

Results and Discussion

Two new *meta* isomers, MnTE-3-PyP and MnTnPr-3-PyP, were synthesized and characterized by elemental analysis, uv/vis spectroscopy, ESI-MS, electrochemistry ($E_{½}$), lipophilicity (R_f and P_{OW}) and SOD-like activity (k_{cat}) (Table 1 and 1S). There are no significant differences in the uv/vis spectral properties of new compounds (see Experimental and Table 1S) relative to other *meta* analogues.[19] The ESI-MS spectral pattern, given in

NIH-PA Author Manuscript

NIH-PA Author Manuscript

NIH-PA Author Manuscript

Experimental, was similar to that described previously for the *ortho* methyl and ethyl analogues.[26] Elemental analyses (Experimental) are consistent with the hydrated species.

Dependence of the $Mn^{III}P/Mn^{II}P$ reduction potential ($E_{½}$) and the SOD activity (k_{cat}) on the number of C atoms in the N-alkylpyridyl chains

The lengthening of the *ortho* alkyl groups influences dramatically solvation and stericity of the porphyrin, which, in turn, affects $E_{½}$ and k_{cat}, as previously discussed in details.[19] Briefly, as the alkyl chain grows from 1 to 8 carbon atoms, due to the increasingly less solvated, thus more exposed positive charges on pyridyls, the $E_{½}$ grows approximately linearly from +220 to +367 mV *vs* NHE (Table 1). However, the dependence of k_{cat} on the number of carbons reveals a delicate balance between two antagonistic factors: the increase of steric hindrance, i. e. crowding near the Mn site, which would decrease k_{cat}; and the increase of the $Mn^{III}P/Mn^{II}P$ reduction potential ($E_{½}$), which is a surrogate for the driving-force of the electron transfer and would increase k_{cat}. Accordingly, k_{cat} first decreases from methyl to butyl as the steric hindrance to the approach of $O_2^{\cdot-}$ to the Mn site increases, but then increases as the favorable thermodynamics for the dismutation reaction ($E_{½}$) predominates (Table 1› Figure 1).[19] The maximum change in $E_{½}$ is 147 mV, and in k_{cat} 0.54 log units (Table 1).

When the alkyl side chains are located in the *meta* positions, farther from the porphyrin core, free rotation of the pyridyl groups is allowed, and the steric and the solvation effects are, thus, much less pronounced. Consequently, the maximum change in $E_{½}$ for the *meta* series is only 14 mV, and for k_{cat} only 0.08 log units (Figure 1). As the alkyl chain lengthens, $E_{½}$ continuously increases (Table 1, Figure 1). For small alkyl side chains, the favorable thermodynamics dominates and an initial small increase in k_{cat} is observed. As the alkyl chains lengthen further (from n-butyl on), the steric hindrance prevails over the increase in $E_{½}$, and k_{cat} starts to decrease. As a result of such trends the SOD activity of some members of the *meta* series is close to the respective analogues in the *ortho* series; this happens for example for the n-propyl and n-butyl compounds where the SOD activities of the respective *ortho* and *meta* isomers approach each other (Figure 1, Table 1). It is worthwhile noting, however, that while the k_{cat} of the *ortho* n-propyl and *ortho* n-butyl compounds are only about 4.9- and 3.6-fold higher than that of their *meta* analogues, the lipophilicity of the *meta* isomers remains 10-fold bigger throughout the series (Table 1).[17] Therefore, due to the interplay of antioxidant potency and lipophilicity some members of the *meta* series may be of identical or higher efficacy than *ortho* isomers in *in vivo* models of oxidative stress. To explore such assumption we studied here the accumulation and the efficacy of both isomeric series in protecting SOD-deficient *E. coli*.

SOD-deficient E. coli (JI132) growth. Efficacy of MnP

The JI132 strain lacks two cytoplasmic SODs, FeSOD and MnSOD, and thus displays phenotypic defects attributable to the damage of important cellular components by superoxide.[27–30] Among those phenotypic deficiencies is the inability to grow aerobically in minimal glucose medium.[29] Only compounds that are potent, cell-permeable SOD mimics, can exert protection, thus restoring the aerobic growth in minimal medium.[31] Our data show that *ortho* and *meta* isomers protect SOD-deficient *E. coli* with nearly equal efficacy (Figure 2). The *meta* and *ortho* ethyl, n-propyl and n-butyl porphyrins appear of nearly identical efficacy at higher concentrations (10 and 20 μM), but *meta* analogues and most so the more lipophilic n-propyl and n-butyl porphyrins are more efficacious than *ortho* analogues at lower concentrations (1 and 5 μM), presumably due to their faster cellular uptake (Figure 2, and 1S). The structural flexibility of the *meta* isomers, that allows them to change their shape and size while crossing the membranes, is difficult to quantify but likely contributes to their high efficacy. Our data suggest that the shorter and the more planar methyl analogue,

NIH-PA Author Manuscript

NIH-PA Author Manuscript

NIH-PA Author Manuscript

MnTM-3-PyP becomes somewhat less efficient at 10–30 μM levels presumably due to the enhanced unfavorable interactions with nucleic acids.[18] The more lipophilic MnTnBu-3-PyP, that also possesses significant surfactant character and can thus disturb the cell membranes, becomes toxic at concentrations ≥20 μM. MnTnHex-3-PyP of even stronger surfactant character is toxic at all concentrations studied; its *ortho* analogue is only slightly less toxic (Figure 2A); this is in agreement with our previous *E. coli* study on *ortho* Mn(III) *N*-alkylpyridylporphyrins.[18]

Toxicity of MnP to wild type E. coli, AB1157

Further assessment of MnP toxicity was accomplished by monitoring their effect on the growth of AB1157, in complete, M9CA medium. None of the Mn porphyrins exerted toxicity at concentrations at which they protected the SOD-deficient JI132 strain (Figure 2S. At higher concentrations, however, the same trend in toxicity, as observed with the growth of JI132, was seen with AB1157 in M9CA medium. MnTM-3-PyP, and more so MnTnBu-3-PyP, exerted toxicity at ≥100 μM (Figure 2AS). Both hexyl analogues accumulate to the highest degree in cytosol and membranes (Figure 3) and exert toxicity at concentrations ≥ 1 μM (Figure 2BS). No toxicity of Mn porphyrins to AB1157 (alkyl = methyl to n-butyl) was observed in 5 amino acid minimal medium at 20 μM levels (Figure 3S).

Accumulation of porphyrins

Accumulation of MnPs in cytosolic (Figure 3) and membrane fractions (Figure 5S) was assessed in both AB 1157 and JI132 *E. coli*. Both strains show similar MnP accumulation profile, but on average the absolute uptake of MnPs is higher in the JI132 strain; this is clearly visible with the hexyl analogues and may be driven by a general *E. coli* attempt to accumulate nutrients or biologically relevant compounds that are neither produced within nor readily available. Since the SOD-deficient *E. coli* strain lacks two cytosolic superoxide dismutases, accumulation of SOD mimics in the cytosol is essential for protecting SOD-deficient mutant. The levels of porphyrins within cytosol and membrane (Figures 3 and 5S) were quantified by using calibration curves for *ortho* and *meta* isomeric porphyrins, where area below porphyrin Soret band was plotted *vs* porphyrin concentration (Figure 4S). Two major findings, depicted in Figures 3 are: (**1**) Compared to *ortho* analogues, *meta* isomers accumulate to significantly higher levels in the cytosol of both strains; due to the more planar structure (conformationally flexible) and higher lipophilicity they cross membrane easier, which apparently overcomes the inferior thermodynamics of *meta* isomers for $O_2^{\cdot -}$ dismutation, contributing at least in part to their high efficacy in substituting for deficiency in both cytosolic SODs. Consequently, the efficacy of *meta* and *ortho* ethyl and n-propyl analogues in *E. coli* study are nearly identical. (**2**) *Ortho* and *meta* hexyl analogues, which possess strong micellar character, accumulate much more than any other porphyrin in cytosol and membranes (Figures 3 and 5S), which seems to compromises membrane structure and its functions.

Although *meta* and *para* isomers have similar $E_{½}$ and SOD activity, the systematic experimentation with the *para* isomers has remained on hold. Due to their conformational flexibility *para* isomers adopt planar structures and thus interact extensively with nucleic acids,[15] which not only results in high toxicity, but also prevents the approach of superoxide to the Mn site;[15] this in turn suppresses their effects in protecting SOD-deficient *E. coli*.[15] The bulkiness of the *ortho* and *meta* isomers prevents such associations to a greater degree.[18] In lights of the finding in the *ortho* and *meta* series described here, longer alkyl *para* analogues may be bulky enough to overcome possible nucleic acid intercalation and further studies with bulkier *para* isomers may thus be warranted.

NIH-PA Author Manuscript

NIH-PA Author Manuscript

NIH-PA Author Manuscript

Experimental Section

Experimental details are given in Supplemental Information. ***General.*** All chemicals are of highest purity and obtained from same commercial sources as indicated before. ***Porphyrins. Elemental analysis*** (Atlantic MicroLab, Norcross, GA): H_2TE-3-PyPCl$_4$·11H_2O. ($C_{48}H_{72}N_8O_{11}Cl_4$) Found: C, 53.82; H, 6.21; N, 10.89; Cl, 13.44 Calculated: C, 53.43; H, 6.73; N, 9.39; Cl, 13.14. H_2TnPr-3-PyPCl$_4$·16H_2O ($C_{52}H_{90}N_8O_{16}Cl_4$) Found: C, 50.98; H, 5.78; N, 9.32; Cl, 11.75 Calculated: C, 50.98; H, 7.40; N, 9.15; Cl, 11.58. MnTE-3-PyPCl$_5$·8.5H_2O ($MnC_{48}H_{61}N_8O_{8.5}Cl_5$) Found: C, 51.74; H, 5.13; N, 9.93; Cl, 16.53 Calculated: C, 51.56; H, 5.50; N, 10.02; Cl, 15.85. MnTnPr-3-PyPCl$_5$·10H_2O ($MnC_{52}H_{76}N_8O_{10}Cl_5$) Found: C, 51.39; H, 6.01; N, 9.22; Cl, 14.31 Calculated: C, 51.05; H, 6.43; N, 9.16; Cl, 14.49. Compounds are ≥98% pure. ***Electrospray ionization mass spectrometric analyses*** (ESI-MS) of 5 μM MnP in a H_2O-acetonitrile (1:1, v/v; containing 0.1 % v/v HFBA) were done as described elsewhere.[26] The m/z peak assignments are consistent with the following species in the given order: [MnT(alkyl)-3-PyP^{5+} + 2HFBA$^-$]$^{3+}$/3), [MnT(alkyl)-3-PyP^{5+} + HFBA$^-$ − 2H$^+$]$^{2+}$/2, [MnT(alkyl)-3-PyP^{5+} + 2HFBA$^-$ − H$^+$]$^{2+}$/2 and [MnT(alkyl)-3-PyP^{5+} + 3HFBA$^-$]$^{2+}$/2. MnTE-3-PyPCl$_5$: Found 404.7 499.3, 606.3, 713.6, Calculated: 404.6, 499.3, 499.3, 606.3, 713.5; MnTnPr-3-PyPCl$_5$, Found: 423.7, 527.5, −, 741.5, Calculated: 423.4, 527.6, 634.6, 741.6. ***UV/vis spectra*** were recorded in H_2O at room temperature (25 ± 1°C). The λ(nm) of Soret bands and the corresponding molar absorptivities, ε (log values in parentheses) are: H_2TE-3-PyP 417.0(5.52); H_2TnPr-3-PyP 417.0(5.55); MnTE-3-PyP 460.0(5.19); MnTnPr-3-PyP 460.0 (5.14). Other absorption maxima and related ε are in Table 1S. ***Cyclic voltammetry*** was performed as described elsewhere.[26] ***SOD-like activity.*** Determination of the $k_{cat}(O_2^{\cdot-})$ using cyt *c* assay was performed as previously described in details.[1,18]

In vivo studies. E. coli growth

Escherichia coli studies on SOD-deficient JI132 and wild type SOD-proficient strain, AB1157 were performed as described.[31]***Accumulation of Mn porphyrins in E. coli.*** The wild type AB1157 and JI132 were grown in flasks in 10 mL of M9CA medium to a density corresponding to A_{700} ~ 0.6. Five μM Mn porphyrins were then added, and the cells were kept on a shaker for additional 60 minutes. Cells were then rapidly washed with ice-cold PBS, resuspended to a total volume of 1.0 ml and disrupted by sonication. Cytosolic and membrane fractions were separated by centrifugation. The membrane fractions were solubilized in 10% sodium dodecylsulfate for 24 hours and then centrifuged at high speed to remove the unsolubilized material. Spectra were recorded and the absorbances of MnP in cytosolic and membrane fractions measured at their Soret bands.[19] Protein levels were measured by Lowry method.[32] Details on the calculations of the accumulation of porphyrins in cytosolic and membrane fractions are given in Supplemental Information along with related Figures 4S–9S.

Supplementary Material

Refer to Web version on PubMed Central for supplementary material.

Acknowledgments

I.K., J.S.R. and I.B.H. acknowledge support by NIAID U19AI67798-01 and W. H. Coulter Translation Partners Grant Program. I.S. thanks NIH/NCI DCCC Core Grant (5-P30-CA014236-33), and L.B. grant MB03/07 from Kuwait University and HSC Research Core Facility grant GM01/01 and technical assistance of Milini Thomas.

NIH-PA Author Manuscript

NIH-PA Author Manuscript

NIH-PA Author Manuscript

Abbreviations Charges are omitted throughout text

MnTalkyl-2(or 3)-PyP^{5+}	Mn(III) *meso*-tetrakis(*N*-alkylyridinium-2 or 3-yl)porphyrin
M, AEOL10112	alkyl being methyl
E, AEOL10113	ethyl
nPr	n-propyl
nBu	n-butyl
nHex	n-hexyl
nHep	n-heptyl
nOct	n-octyl, 2 and 3 relate to *ortho* and *meta* isomers respectively
AEOL10150	MnTDE-2-ImP, Mn(III) tetrakis(*N*,*N*′-diethylimidazolium-2-yl)porphyrin
R_f	porphyrin path/solvent path
TLC	thin-layer chromatographic retention factor

References

1. Rebouças JS, DeFreitas-Silva G, Idemori YM, Spasojević I, Benov L, Batinić-Haberle I. The impact of electrostatics in redox modulation of oxidative stress by Mn porphyrins. Protection of SOD-deficient *E. coli* via alternative mechanism where Mn porphyrin acts as a Mn-carrier. Free Radic Biol Med 2008;45:201–210. [PubMed: 18457677]
2. Batinić-Haberle I, Benov L, Spasojević I, Hambright P, Crumbliss AL, Fridovich I. The Relationship Between Redox Potentials, Proton Dissociation Constants of Pyrrolic Nitrogens, and *in Vitro* and *in Vivo* Superoxide Dismutase Activities of Manganese(III) and Iron(III) Cationic and Anionic Porphyrins. Inorg Chem 1999;38:4011–4022.
3. Ferrer-Sueta G, Vitturi D, Batinić-Haberle I, Fridovich I, Goldstein S, Czapski G, Radi R. Reactions of Manganese Porphyrins with Peroxynitrite and Carbonate Radical Anion. J Biol Chem 2003;278:27432–27438. [PubMed: 12700236]
4. DeFreitas-Silva G, Rebouças JS, Spasojević I, Benov L, Idemori YM, Batinić-Haberle I. SOD-like activity of Mn(II) β-octabromo-meso-tetrakis(*N*-methylpyridinium-3-yl)porphyrin equals that of the enzyme itself. Arch Biochem Biophys 2008;477:105–112. [PubMed: 18477465]
5. Halliwell, B.; Gutterdige, JMC. Biosciences. Oxford University Press; 2007. Free Radicals in Biology and Medicine.
6. Zhao Y, Chaiswing L, Oberley TD, Batinić-Haberle I, StClair W, Epstein CJ, StClair D. A mechanism-based antioxidant approach for the reduction of skin carcinogenesis. Cancer Res 2005;I: 1401–1405. [PubMed: 15735027]
7. Tse H, Milton MJ, Piganelli JD. Mechanistic analysis of the immunomodulatory effects of a catalytic antioxidant on antigen-presenting cells: Implication for their use in targeting oxidation/reduction reactions in innate immunity. Free Radic Biol Med 2004;36:233–47. [PubMed: 14744635]
8. Sheng H, Sakai H, Yang W, Fukuda S, Salahi M, Day BJ, Huang J, Paschen W, Batinić-Haberle I, Crapo JD, Pearlstein RD, Warner DS. Sustained treatment is required to produce long-term neuroprotective efficacy from a metalloporphyrin catalytic antioxidant in focal cerebral ischemia. Free Radic Biol Med. 2009 in press.
9. Moeller BJ, Cao Y, Li CY, Dewhirst MW. Radiation activates HIF-1 to regulate vascular radiosensitivity in tumors: Role of oxygenation, free radicals and stress granules. Cancer Cell 2005;5:429–441. [PubMed: 15144951]
10. Rabbani ZN, Spasojević I, Vasquez-Vivar J, Haberle S, Dewhirst MW, Vujaskovic Z, Batinić-Haberle I. Anti-tumor Effects of Mn(III) *Ortho* Tetrakis *N*-ethylpyridylporphyrin, MnTE-2-PyP^{5+}

NIH-PA Author Manuscript

NIH-PA Author Manuscript

NIH-PA Author Manuscript

in Mice Model of Breast Tumor *Via* Suppression of Tumor Oxidative Stress. Free Radic Biol Med. 2009 under revision.

11. Moeller BJ, Batinić-Haberle I, Spasojević I, Rabbani ZN, Anscher MS, Vujaskovic Z, Dewhirst MW. A manganese porphyrin superoxide dismutase mimetic enhances tumor radioresponsiveness. Int J Rad Oncol Biol Phys 2005;63:545–552.
12. Gauter-Fleckenstein B, Fleckenstein K, Owzar K, Jian C, Batinić-Haberle I, Vujaskovic Z. Comparison of two Mn porphyrin-based mimics of superoxide-dismutase (SOD) in pulmonary radioprotection. Free Radic Biol Med 2008;44:982–989. [PubMed: 18082148]
13. Piganelli JD, Flores SC, Cruz C, Koepp J, Young R, Bradley B, Kachadourian R, Batinić-Haberle I, Haskins K. A Metalloporphyrin Superoxide Dismutase Mimetic (SOD Mimetic) Inhibits Autoimune Diabetes. Diabetes 2002;51:347–355. [PubMed: 11812741]
14. Batinić-Haberle I, Ndengele MM, Cuzzocrea S, Rebouças JS, Spasojević I, Salvemini D. Lipophilicity is a critical parameter that dominates the efficacy of metalloporphyrins in blocking morphine tolerance through peroxynitrite-mediated pathways. Free Radic Biol Med 2009;46:212–219. [PubMed: 18983908]
15. Rebouças JS, Spasojević I, Tjahjono DH, Richaud A, Mendez; F, Benov L, Batinić-Haberle I. Redox modulation of oxidative stress by Mn porphyrin-based therapeutics: The effect of charge distribution. Dalton Trans 2008:1233–1242.
16. Saba H, Batinić-Haberle I, Munusamy S, Mitchell T, Lichti C, Megyesi J, MacMillan-Crow LA. Manganese porphyrin reduces renal injury and mitochondrial damage during ischemia/reperfusion. Free Radic Biol Med 2007;42:1571–1578. [PubMed: 17448904]
17. Kos I, Rebouças JS, DeFreitas-Silva G, Vujaskovic Z, Dewhirst MW, Spasojević I, Batinić-Haberle I. The effect of lipophilicity of porphyrin-based antioxidants. Comparison of ortho and meta isomers of Mn(III) N-alkylpyridylporphyrins. Free Radic Biol Med 2009;47:72–78. [PubMed: 19361553]
18. Batinić-Haberle I, Benov L, Spasojević I, Fridovich I. The *Ortho* Effect Makes Manganese (III) *Meso*-Tetrakis(*N*-methylpyridinium-2-yl)Porphyrin (MnTM-2-PyP) a Powerful and Potentially Useful Superoxide Dismutase Mimic. J Biol Chem 1998;273:24521–24528. [PubMed: 9733746]
19. Batinić-Haberle I, Spasojević I, Stevens RD, Hambright P, Fridovich I. Manganese(III) *meso*-tetrakis *ortho N*-alkylpyridylporphyrins. Synthesis, characterization and catalysis of $O_2^{\bullet-}$ dismutation. J Chem Soc, Dalton Trans 2002:2689–2696.
20. Okado-Matsumoto A, Batinić-Haberle I, Fridovich I. Complementation of SOD-deficient Escherichia Coli by manganese porphyrin mimics of superoxide dismutase activity. Free Radic Biol Med 2004;37:401–10. [PubMed: 15223074]
21. Wise-Faberowski L, Warner DS, Spasojević I, Batinić-Haberle I. The effect of lipophilicity of Mn (III) *ortho N*-alkylpyridyl- and di*ortho N, N′*-imidazolylporphyrins in two *in-vitro* models of oxygen and glucose deprivation -induced neuronal death. Free Radic Res 2009;43:329–339. [PubMed: 19259881]
22. Pollard J, Rebouças JS, Durazo A, Kos I, Fike F, Panni M, Gralla EB, Valentine JS, Batinić-Haberle I, Gatti RA. Radioprotective effects of manganese-containing superoxide dismutase mimics on ataxia telangiectasia cells. Free Radic Biol Med 2009;47:250–260. [PubMed: 19389472]
23. Tan S, Batinić-Haberle I. MnTnHex-2-PyP in rabbit cerebral palsy model. unpublished.
24. Szabó C, Mabley JG, Moeller SM, Shimanovich R, Pacher P, Virag L, Soriano VG, van Duzer JH, Williams W, Salzman AL, Groves JT. Pathogenic Role of Peroxynitrite in the Development of Diabetes and Diabetic Vascular Complications: Studies with FP15, a Novel Potent Peroxynitrite Decomposition Catalyst. Mol Med 2002;8:571–580. [PubMed: 12477967]
25. Saltsman I, Botoshansky M, Gross Z. Facile synthesis of ortho-pyridyl-substituted corroles and molecular structures of analogues porphyrins. Tetrahedron Lett 2008;49:4163–4166.
26. Rebouças JS, Spasojević I, Batinić-Haberle I. Quality of Mn-porphyrin-based SOD mimics and peroxynitrite scavengers for preclinical mechanistic/therapeutic purposes. J Pharm Biomed Anal 2008;48:1046–1049. [PubMed: 18804338]
27. Imlay JA. Cellular defenses against superoxide and hydrogen petoxide. Annu Rev Biochem 2008;77:755–776. [PubMed: 18173371]

NIH-PA Author Manuscript

NIH-PA Author Manuscript

NIH-PA Author Manuscript

28. Imlay JA. Pathways of oxidative damage. Annu Rev Microbiol 2003;57:395–418. [PubMed: 14527285]

29. Carlioz A, Touati D. Isolation of superoxide dismutase mutants in Escherichia coli: is superoxide dismutase necessary for aerobic life? EMBO 1986;5:623–630.

30. Messner KR, Imlay JA. The identification of primary sites of superoxide and hydrogen peroxide formation in the aerobic respiratory chain and sulfite reductase complex of *Escherichia coli*. J Biol Chem 1999;274:10119–10128. [PubMed: 10187794]

31. Batinić-Haberle I, Cuzzocrea S, Rebouças JS, Ferrer-Sueta G, Emanuela Mazzon E, Di Paola R, Radi R, Spasojević I, Benov L, Salvemini D. Pure MnTBAP selectively scavenges peroxynitrite over superoxide: Comparison of pure and commercial MnTBAP samples to MnTE-2-PyP in two different models of oxidative stress injuries, SOD-specific *E. coli* model and carrageenan-induced pleurisy. Free Radic Biol Med 2009;46:192–201. [PubMed: 19007878]

32. Lowry OH, Rosebrough NJ, Farr AL, Randall RJ. Protein measurement with the folin phenol reagent. J Biol Chem 1951;193:265–275. [PubMed: 14907713]

NIH-PA Author Manuscript

NIH-PA Author Manuscript

NIH-PA Author Manuscript

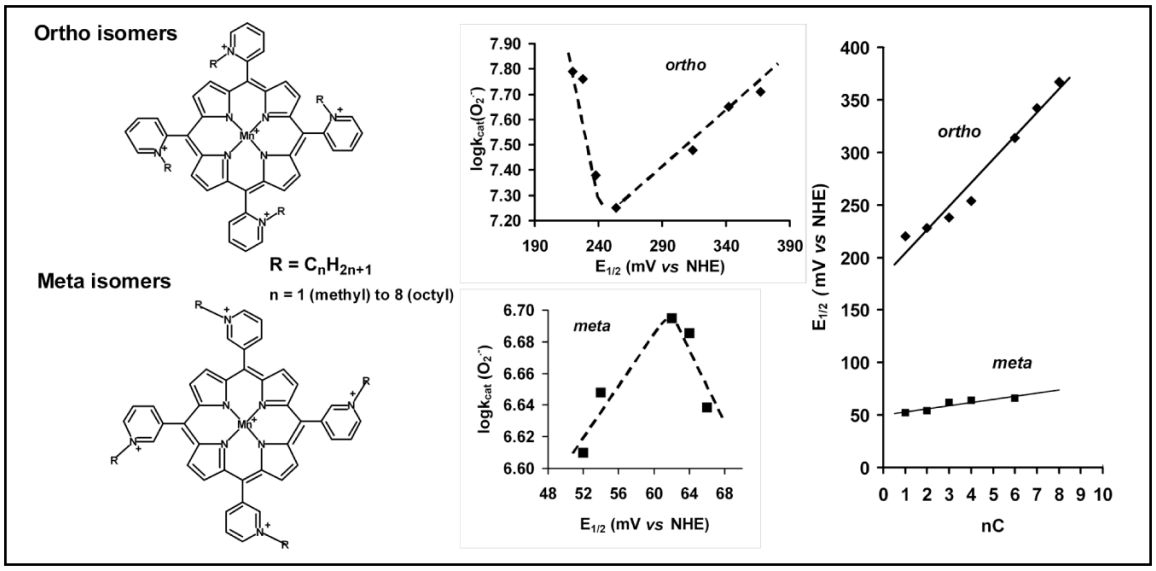

Figure 1.

Structures of *meta* and *ortho* Mn(III) *N*-alkylpyridylporphyrins and the relationships between the log k_{cat} ($O_2^{\cdot-}$) [at (25±1)°C, k_{cat} in $M^{-1}s^{-1}$] and $E_{½}$ ($Mn^{III}P/Mn^{II}P$ redox couple), and $E_{½}$ and the number of carbon atoms (nC) in the alkyl groups (R) of isomers.

NIH-PA Author Manuscript

NIH-PA Author Manuscript

NIH-PA Author Manuscript

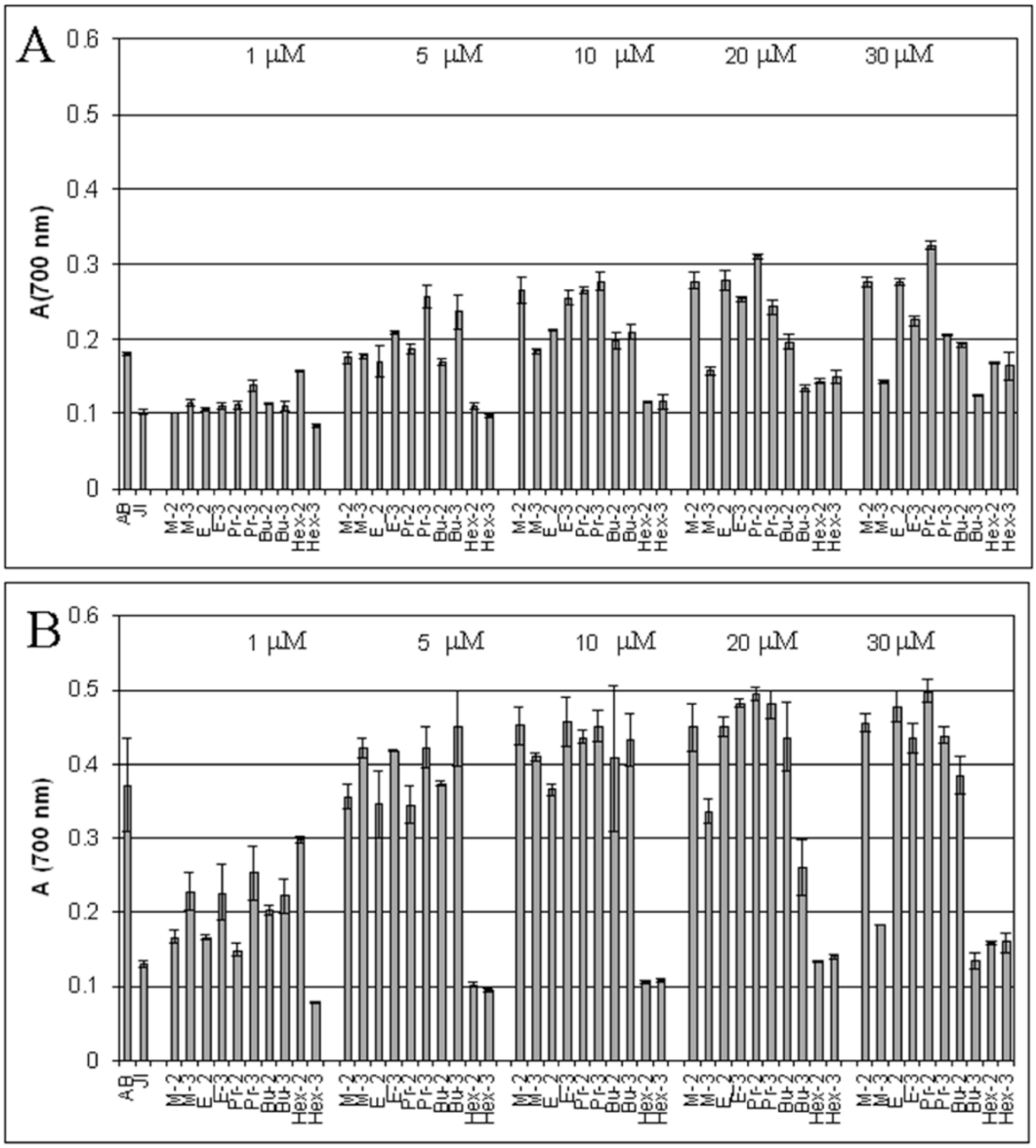

Figure 2.

The aerobic growth of SOD-deficient *E. coli* JI 132 in 5 amino acid minimal medium (absorbance at 700 nm) in the presence of *ortho*(2) and *meta*(3) analogues shown here at 14^{th} (**A**) and 18^{th} hour (**B**)of growth. The growth of SOD-proficient *E. coli* AB1157 is shown also. Bars represent mean ± S.E.

NIH-PA Author Manuscript
NIH-PA Author Manuscript
NIH-PA Author Manuscript

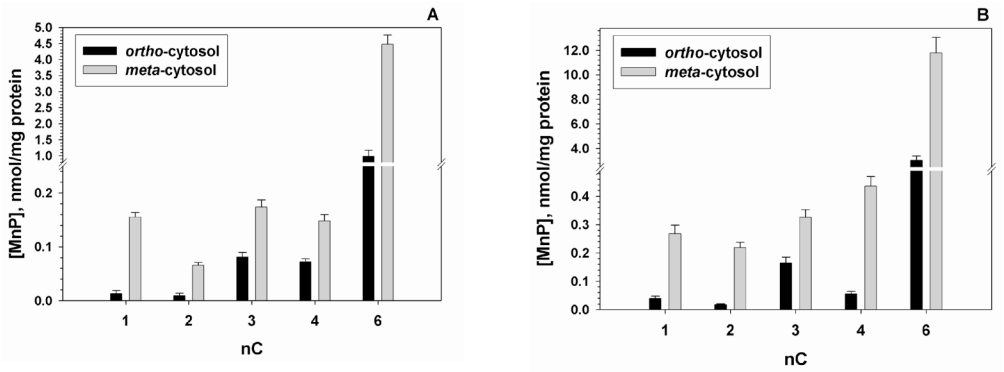

Figure 3.

Accumulation of isomeric Mn(III) *N*-alkylpyridylporphyrins in cytosolic fractions of wild AB1157 (**A**) and SOD-deficient JI132 strain of *E. coli* (**B**). *E. coli* was incubated 1 hour with 5 μM MnP in M9CA medium. Bars represent mean ± S.E. Accumulation in membranes is shown in Supplemental Material, Figures 6S–9S.

NIH-PA Author Manuscript

NIH-PA Author Manuscript

NIH-PA Author Manuscript

Table 1

The lipophilicity expressed as TLC retention factor, R_f (Sigma/Aldrich silica-gel plates with KNO_3-saturated H_2O:H_2O:acetonitrile=1:1:8)[17] and partition between n-octanol and water, P_{OW}[17], k_{cat} for $O_2^{\cdot-}$ dismutation (at (25 ± 1)°C, 0.05 M phosphate buffer, pH 7.8), [2,18,19], and this work and the metal-centered reduction potential for $Mn^{III}P/Mn^{II}P$ redox couple, $E_{½}$, in mV *vs* NHE (in 0.05 M phosphate buffer, pH 7,8, 0.5mM MnP, 0.1 M NaCl).[2,18,19] and this work

Porphyrin	R_f	log P_{OW}	$E_{½}$	log k_{cat}
MnTM-2-PyP	0.03	−7.86	+220	7.79
MnTE-2-PyP	0.06	−6.89	+228	7.76
MnTnPr-2-PyP	0.11	−5.93	+238	7.38
MnTnBut-2-PyP	0.19	−5.11	+245	7.25
MnTnHex-2-PyP	0.38	−2.76	+314	7.48
MnTnHep-2-PyP	0.46	−2.10	+342	7.65
MnTnOct-2-PyP	0.49	−1.24	+367	7.71
MnTM-3-PyP	0.05	−6.96	+52	6.61
MnTE-3-PyP	0.10	−5.98	+54	6.65
MnTnPr-3-PyP	0.22	−5.00	+62	6.69
MnTnBut-3-PyP	0.40	−4.03	+64	6.69
MnTnHex-3-PyP	0.55	−2.06	+66	6.64